Proceedings of the 15th Meeting on Modelling
of Material Processing with Lasers (M4PL15)
19-21 January 2000, Igls/Innsbruck, Austria

Direct Calculation of Optimized Laser Power Density Profiles for Laser Heating

Gert-Willem R.B.E. Römer[1] and Roelof F. de Graaf[2]

[1]University of Twente, Dept. of Mechanical Engineering
P.O. Box 217, 7500 AE, Enschede, the Netherlands
g.r.b.e.romer@wb.utwente.nl, http://www.wa.wb.utwente.nl

[2]WTCM/CRIF, Campus Arenberg, Celestijnenlaan 300C
3001 Heverlee (Leuven), Belgium
roelof.degraaf@wtcm.be, http://www.wtcm.be

Abstract

Laser surface heating requires a well defined temperature profile. In this paper the inverse problem of heat conduction in solids is solved, based on the two-dimensional Fourier transform. That is, the required power density profile of the laser beam can be calculated directly from a desired temperature field. Problems and errors introduced by calculations on a finite grid and by physically impossible temperature gradients are addressed to.

1 Introduction

The results of laser surface treatment follows from the time-temperature history and is a function of the thermo-physical properties of the material, the velocity of the laser beam relative to the work piece and, most importantly, by the power density profile of the laser beam.

The current practice to establish a desired temperature distribution in the work piece is by an iterative two-step approach, known *beam shaping* [1, 2]. First, the temperature history induced by the power density profile under consideration is determined, either by process modelling or by experiments. In the second step, the power density profile is modified such that its corresponding temperature history approaches the desired temperature history. This method may require several iteration steps, which depends on subjective modifications of the power density profile by the laser engineer, and may result in a sub-optimal power density distribution.

It will be shown that the optimal power density profile can be directly calculated from the desired temperature distribution, when assuming no melting, constant beam velocity and constant thermo-physical properties [3–5]. This solution of the *inverse heat conduction problem* is based on the two-dimensional Fourier transform and is discussed in the next section. A method to reduce errors due frequency leakage is addressed to. In addition, a method to keep the solution within the physical constraints is discussed.

2 Calculation of power density profile

2.1 Solution of the inverse heat conduction problem

Assuming constant relative beam velocity v[m/s] in the x-direction, and considering a quasi-stationary situation (i.e. $\lim_{t\to\infty} T$), the temperature history T and the temperature distribution in the work piece, expressed in a coordinate system moving with the laser beam, are related by a simple change of variable $x = vt$, in which t[s] denotes time. The temperature distribution $T(x, y, z)$[K], induced by a laser beam with power density profile $I(x, y)$[W/m^2], moving over the surface of a work piece of semi-infinite dimensions, are related as [6]

$$T(x,y,z) = \int_{-\infty}^{\infty}\int_{-\infty}^{\infty} AI(x',y')W(x-x',y-y',z)dx'dy' \tag{1}$$

where

$$W = \frac{1}{2\pi KR}\exp\left[\frac{-v}{2\kappa}(x-x'+R)\right],\ R = \sqrt{(x-x')^2+(y-y')^2+z^2} \tag{2}$$

with K[W/(m K)] the thermal conductivity of the material, κ[m^2/s], the thermal diffusitivity, and A[$-$] the absorptivity. All these material parameters are assumed to be constant. The temperature distribution T is the excess temperature over the initial T_0[K] of the work piece. The function W[K/W] is the temperature distribution of a point heat source moving over the surface of the semi-infinite work piece [6]. Here z[m] denotes the depth of the xy-plane of interest, and is considered to be constant in the following.

Equation (1) represents a convolution of the power density AI and the function W with respect to the coordinates x and y. That is, $T = AI * W$, where $*$ denotes the convolution operator. Then, by denoting the two-dimensional Fourier transform [7], as $\mathcal{F}_2\{G\} = \tilde{G}$, equation (1) can be rewritten as

$$\mathcal{F}_2\{T\} = \mathcal{F}_2\{AI * W\} \Leftrightarrow \mathcal{F}_2\{T\} = A\mathcal{F}_2\{I\}\mathcal{F}_2\{W\} \Leftrightarrow \tilde{T} = A\tilde{I}\,\tilde{W} \tag{3}$$

where the well known Fourier equality $\mathcal{F}_2\{F * G\} = \mathcal{F}_2\{F\}\mathcal{F}_2\{G\}$ was used. Rewriting equation (3) yields

$$\tilde{I} = \frac{1}{A}\frac{\tilde{T}}{\tilde{W}} \tag{4}$$

The power density corresponding to a given temperature distribution T can now be calculated from

$$I = \frac{1}{A}\mathcal{F}_2^{-1}\left\{\frac{\tilde{T}}{\tilde{W}}\right\} \tag{5}$$

where $\mathcal{F}_2^{-1}\{\cdot\}$ denotes the inverse Fourier transform.

2.2 Numerical evaluation

By replacing the continuous convolution by discrete convolution, the power density profile can be calculated numerically using the two-dimensional Fast Fourier Transform (FFT) algorithm. On an equidistant grid of $N \times N$ points in the xy-plane, with dimensions L[m]$\times L$ [m] (see figure 1), this

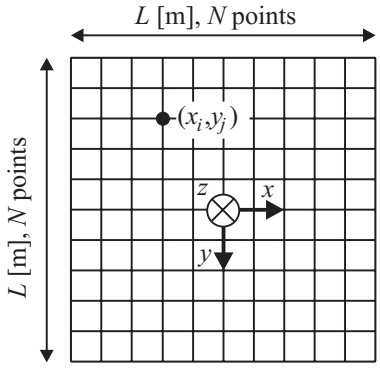

Figure 1: Square grid of $N \times N$ equidistant points in the xy-plane on which the desired temperature distribution and function W are considered as piece wise constant.

requires $O(N^2)$ operations. As R is a factor in the denominator of the function W (2) it represents a singularity, which causes numerical problems if $R \approx 0$. In that case the function W should be replaced by W_0, which is defined by [5]

$$W_0 = \frac{1}{2\pi K \Delta x \Delta y} \exp\left(-\frac{vz}{2\kappa}\right) \times \left[\Delta x \ln\left(\frac{w_1 + \Delta x}{w_1 - \Delta x}\right) + \Delta y \ln\left(\frac{w_2 + \Delta y}{w_2 - \Delta y}\right) - 4z\left(\tan^{-1}\left(\frac{w_1}{2z}\right) + \tan^{-1}\left(\frac{w_2}{2z}\right)\right) + 2z\pi\right] \tag{6}$$

where $\Delta x = \Delta y = L/(N-1)$ in the case of an equidistand grid and

$$w_1 = \sqrt{\frac{\Delta x^2 + 4z^2\cos^2\beta}{\sin^2\beta}},\ w_2 = \sqrt{\frac{\Delta y^2 + 4z^2\sin^2\beta}{\cos^2\beta}},\ \beta = \tan^{-1}\left(\frac{\Delta y}{\Delta x}\right) \tag{7}$$

In the case $z = 0$ as well as $R \ll 1$, function W should be replaced by $\lim_{z\to 0} W_0$.

2.3 Example

The desired temperature distribution is selected from the temperature-time-transformation diagram to be, in the case of C45 steel , above 1200°C to obtain homogeneous austenite on the surface within 0.5s. This corresponds to a maximum surface hardness of 840Hv [8]. At deeper layers the temperature is lower, resulting in inhomogeneous austenite, which in turn results in lower hardness, depending on the original grain structure. Here, $T_{\text{depth}} \geq$950°C is specified for adequate hardness ($\geq$700Hv). From simulations it was found that the optimum temperature distribution was a square distribution with a maximum temperature of 1350°C. A higher temperature will result in deeper hardening for this material, but surface melting might occur, especially when an absorbing graphite coating reduces the melting temperature. A different distribution was required for a hyper-eutectic 100Cr6 ball bearing steel. Here, the surface temperature should not exceed 1100°C to obtain a maximum hardness of 900Hv, while at hardening depth the temperature should be preferably over 1000°C. Figure 2(a) was optimized for this case. Figure 2(b) shows the power density profile as calculated by applying (5).

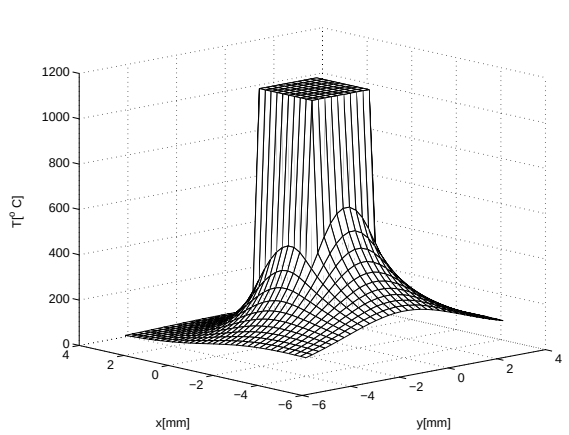

(a) Desired temperature distribution for laser transformation hardening of 100Cr6 steel, at 5mm/s.

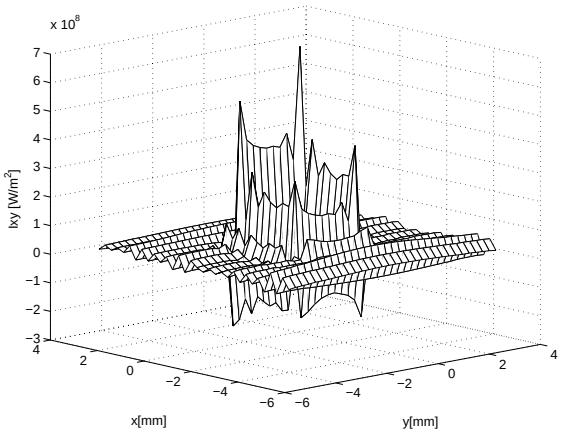

(b) Laser beam power density profile, corresponding to the temperature distribution to the left.

Figure 2: Example of equation (5) applied to laser transformation hardening, $N = 32$.

3 Calculation errors

Analysis of the power density profile in Figure 2(b) shows some ripples, which are introduced by the Fourier transformation. In addition, negative power densities near the central lobe of the power density are observed. Both phenomena are discussed in the following.

3.1 Frequency leakage

The ripples in the power density profile are most significant at the boundaries of the grid, especially at $x(\pm L/2)$. They result from the truncation of the functions T and W at the boundary of the grid, combined with the fact that a discrete Fourier transform (FFT) is used. The discrete Fourier transform assumes that the (truncated) functions repeat periodically [9], see figure 3(a). The start and the end of functions T and W are not continuous, and a fictitious jump is present in the functions. These jumps cause a distortion of the corresponding frequency spectra $\tilde{T}$ and $\tilde{W}$, known as *frequency leakage* or *boundary effect* or *overspill*. Frequency leakage introduces ripples after inverse Fourier transformation. The boundary effect can be reduced by increasing the dimensions $L \times L$ of the grid. In that case the amplitude of the fictitious jumps will decrease, because for $\sqrt{x^2 + y^2} \to \infty$, $T \to 0$ and $W \to 0$. As a results frequency leakage and ripples in the density profile will decrease. This approach requires more computation time.

The boundary effect can also be reduced by windowing. Windows are multiplicative weighting functions $f(x, y)$[-], which reduce the order of discontinuity at the boundaries of the grid by forcing the functions T and W, and their derivatives, to zero at the boundaries of the grid*. Windowing the functions T and W prior to Fourier transformation reduces the ripples, but causes a distortion of the frequency spectra. However, appropriate selection of the window function reduces the ripples in the power density profile, without significantly distorting the frequency spectrum. Popular window functions (such as those of *Bartlett*, *Blackman*, *Hamming*, *Hanning*, *Kaiser* and *Welch*) are available from literature [9]. It was found that the following windowing function produces the

*Note that the truncation of the functions T and W, as was applied in figure 2(a), and figure 3(a), corresponds to a window function $f(x, y) = 1 \; \forall (x, y) \in [-L/2, L/2] \times [-L/2, L/2]$.

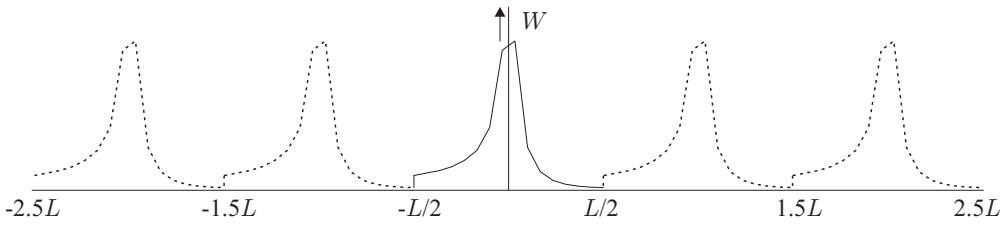

(a) Truncated function, which corresponds to windowing with $f(x, y) = 1$ for all nodes on the grid.

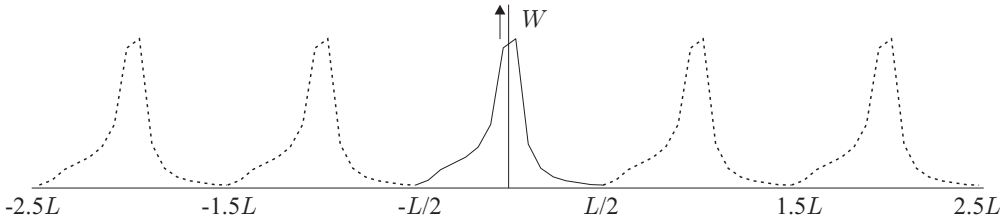

(b) After windowing with equation (8).

Figure 3: Section along the x-axis of function W in 100Cr6 and its periodic extension under discrete Fourier transform (N=16).

best results

$$f(x) = \begin{cases} \cos\left[(|x| - r_x)/(1 - r_x)\pi\right] & \text{if } |x| < r_x \\ 1 & \text{elsewhere} \end{cases} \tag{8}$$

in which $r_x = 2\sqrt{\sigma_x^2}$ denotes the radius of the function to be windowed, and σ_x^2 its second moment (variance) in the x-direction. A similar function was applied for the y-dimension. Figure 3(b) shows the W function after windowing was applied. Figure 4 shows the power density profile after applying windowing to the functions T and W. The ripples in the profile are significantly reduced.

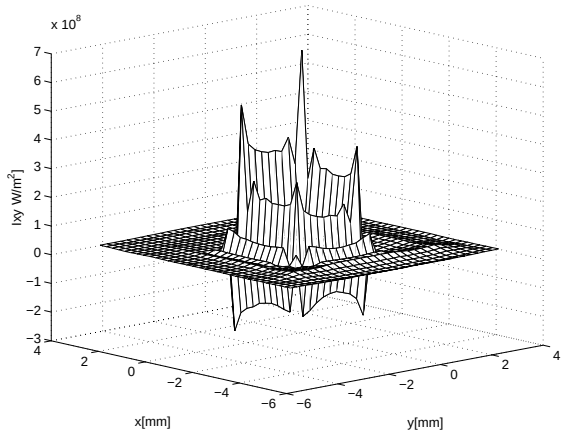

Figure 4: Power density profile corresponding to temperature distribution of figure 2(a), after windowing of T and W with equation (8).

3.2 Negative intensities

The power density profile of figure 2(b) as well as in figure 4 show some locations of negative energy. Negative power densities are required to produce steep temperature gradients $\partial T/\partial x$ and $\partial T/\partial y$. Negative intensities are obviously physically impossible. The maximum attainable temperature gradients are constrained by the thermal diffusitivity κ of the material and the beam velocity. The negative power densities are not the result of the use of the (discrete) Fourier transform. Therefore, the calculation method can not be modified such that it produces positive intensities only. That is, in the case of negative intensities, the desired beam velocity should be reduced or the desired temperature distribution should be redefined. However, in some cases the sum of negative energy is small. Figure 5 shows the effect of zeroing the negative intensities on the temperature distribution.

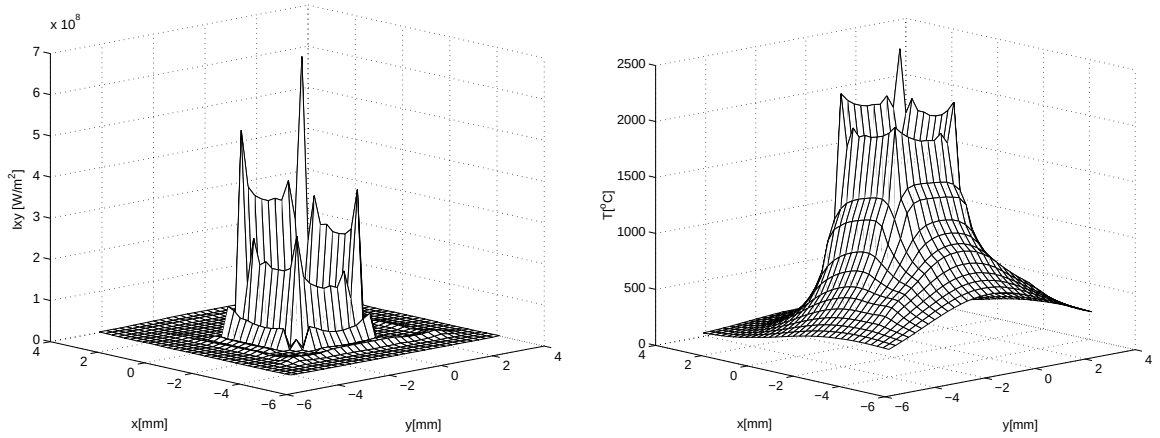

(a) Power density profile as calculated by applying windowing and zeroing the negative intensities.

(b) Surface temperature distribution caused by power density profile of figure 5(b).

Figure 5: Power density profile and corresponding temperature distribution in 100Cr6, v=5mm/s, N=32.

4 Optimization of power density profiles

As can be seen in figure 5(a), the calculated power density distribution still contains spikes, which are hard to realize by the use of passive optical components. Moreover, due to the cancellation of the negative intensities, the maximum temperature is too high (compare figures 2(a) and 5(b)). Therefore the calculated power density distribution needs some optimization. For that purpose, an object function, to evaluate the resulting temperature field at depth z, is required

$$\mathcal{O} = \frac{1}{N^2} \sum_{\forall x} \sum_{\forall y} \left[T_{\text{desired}}(x, y, z) - T_{\text{calculated}}(x, y, z) \right]^2 \tag{9}$$

The temperature distribution $T_{\text{calculated}}$, corresponding to a given power density profile I, can also be calculated using the two-dimensional Fourier transform. That is, it follows from (3)

$$T_{\text{calculated}} = A \mathcal{F}_2^{-1} \{ \tilde{I} \tilde{W} \} \tag{10}$$

which requires $O(N^2)$ operations. Applying the Fourier transform to calculate the temperature distribution is significantly more efficient than by *multi-summation*, in which the integrals of (1) are replaced by summations. This would require $O(N^4)$ operations [10]. It is also more efficient than *Multi-grid Multi-level integration* [11], which would require $O(N^2 \log N^2)$ operations.

Several methods are available to perform optimizations of the power density profile. Two methods are discussed in more detail. First, the method of *simulated annealing* will be discussed. Next, spatial filtering of the power density profile as calculated method described in section 2, is discussed.

4.1 Simulated annealing

Simulated annealing [12] has been proven rather successful in optimizing *NP-complete* problems, like the classical traveling salesman problem. At the heart of the method of simulated annealing is an analogy with thermodynamics, specifically with the way that liquids freeze and crystallize, or metals cool and anneal. At high temperatures, the molecules of a liquid move freely with respect to one another. If the liquid is cooled slowly, thermal mobility is lost. The atoms are often able to line themselves up and form a pure crystal that is completely ordered. This crystal represents the state of minimum energy. For slowly cooled systems, nature is able to find this minimum energy state. In fact, if a liquid metal is cooled quickly, it does not reach this state, but rather ends up in an amorphous state having somewhat higher energy.

In the method of simulated annealing, random changes of the power density profile (increasing or decreasing intensity at grid points) are proposed repeatedly. The resulting temperature field is evaluated using equation (9). If the result has improved, the proposed changes will be accepted. If the result did not improved, then the acceptance of the proposed changes will be decided on by chance. The probability of the acceptance will diminish in time. Like in slow crystallization, local minima can be avoided in this way.

However, it was found that using simulated annealing for optimizing the power density profile does not produce acceptable results. Minimizing the object function $\mathcal{O}$ (9), results in a power density distributions with numerous spikes, see figure 6. Such a spiky power density profile may

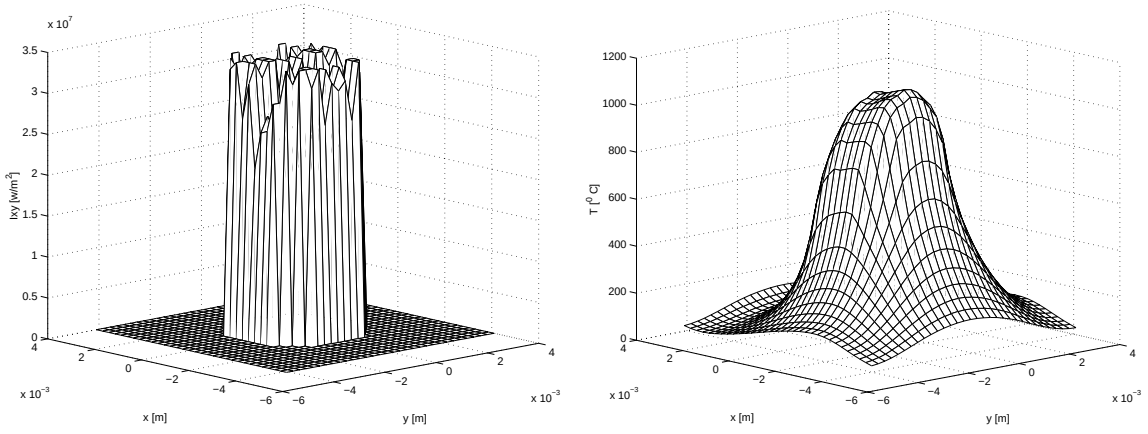

(a) Power density profile, $\mathcal{O} = 106.3$ after 61 iterations.

(b) Temperature distribution corresponding to figure 6(a).

Figure 6: Results obtained by simulated annealing, 100Cr6, v=5mm/s, N=32, initial power density profile: tophat, 500W, 4mm diameter, $\mathcal{O} = 308.3$.

yield a small value of $\mathcal{O}$, because heating of a work piece with a moving laser beam can be considered as an integrating operation, with respect to the density profile. That is, equation (1) with function W represents a low pass operation on the density profile. This implies that a spiky profile may result in a temperature distribution, which approximates the desired distribution quite well (small value of $\mathcal{O}$), provided that the total power and dimensions of the spiky profile match with the optimal profile. This conclusion has two important implications: (*i*) first, minute beam shaping is not advantageous, due to the integrating character of the heat diffusion process, (*ii*) secondly, when the optimized density profile should contain positive intensities only, there is no unique answer to the question what the power density distribution should look like, in order to obtain a certain temperature field. That is, additional constrains are required to obtain a properly posed problem.

Hence, there is no need to develop advanced and expensive optical designs to realize spiky profiles, because a much simpler design (producing a less spiky profile) will perform probably just as well. This fact can be used in the composition of the additional constrains for the optimization problem. The requirement not to induce (surface) melting could be incorporated into these additional requirements. And all the possible solutions should be evaluated at their economical costs.

4.2 Spatial filtering of the calculated density profile

The concept of non-uniqueness of the positive power density profile led to the idea to take the density profile as calculated by the method, discussed in section 2, and use it as the initial profile for an optimization routine in which the profile is adjusted by *spatial filtering*.

The problem of the spikyness of the profile can be resolved by repeatedly applying a spatial filter to the power density profile. It was found that the spatial filter, defined by the matrix

$$\frac{1}{8}\begin{bmatrix} 0 & 1 & 0 \\ 1 & 4 & 1 \\ 0 & 1 & 0 \end{bmatrix} \tag{11}$$

produced the best results. This matrix is convolved with every grid point of the power density distribution. This means that every grid point is averaged with its neighbors, although the emphasis remains on the grid point itself.

The problem of the incorrect maximum temperature (compare figures 2(a) and 5(b)) can be resolved linearly adjustment of the total power level of the density profile according to the ratio between the maximum desired temperature and the maximum calculated temperature. As a result, the value of the object function $\mathcal{O}$ will be increased slightly by this operation, but the obtained power density distribution will be more feasible.

Figure 7 shows the results after one and ten passes of the spatial filter, both with adjustment of the total power. It can be observed that spatial filtering results in a smooth power density profile. The corresponding temperature distribution is hardly affected by this smoothing operation.

5 Conclusions

It was shown that the optimal power density profile can be directly calculated from the desired temperature distribution, when assuming no melting, constant beam velocity and constant thermophysical properties. This solution of the *inverse heat conduction problem* is based on the two-dimensional Fourier transform.

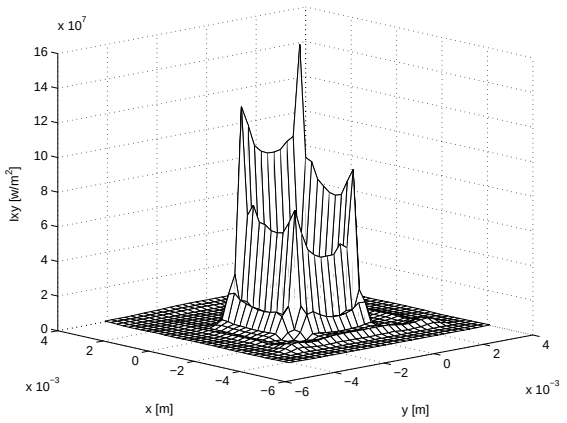

(a) Power density profile of figure 5(a) after one filter and power adjustment pass, $\mathcal{O} = 25.7$.

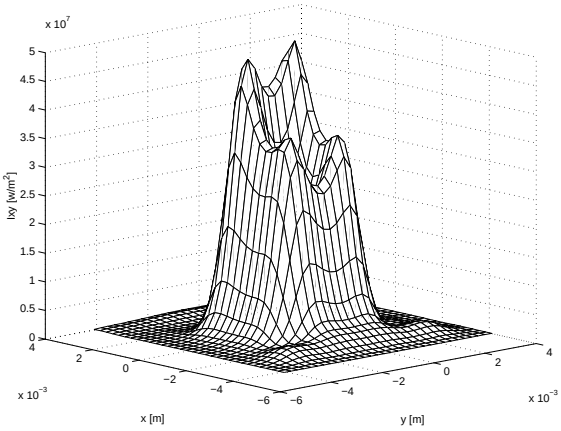

(b) Power density profile of figure 5(a) after ten filter and power adjustment passes, , $\mathcal{O} = 36.8$.

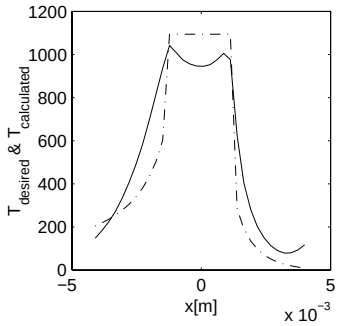

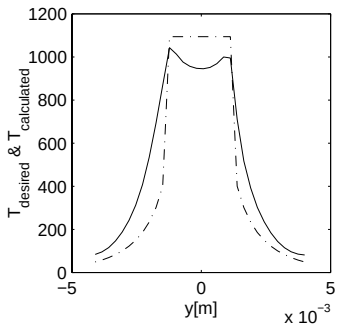

(c) Temperature distribution (solid curve) corresponding to figure 7(a) compared with the desired temperature distribution (dashed).

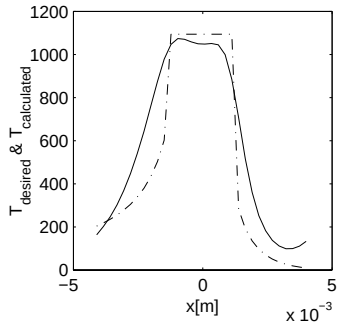

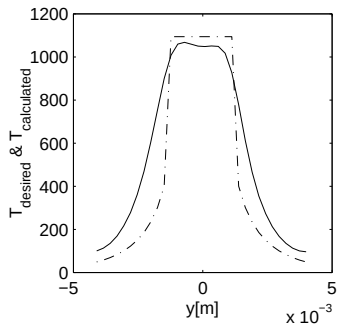

(d) Temperature distribution (solid curve) corresponding figure 7(b) compared with the desired temperature distribution (dashed).

Figure 7: Power density profile and corresponding temperature distribution in 100Cr6 after spatial filtering and power adjustment, v=5mm/s, N=32.

The numerical evaluation of the power density profile may show ripples, introduced by truncation of the functions to be transformed. To suppress ripples the grid size should be increased or windowing should be applied. The method can not be adjusted such that it produces a density profile with positive intensities. These negative intensities are the result of steep gradients in the desired temperature profile. If negative intensities occur, the desired temperature profile should be reformulated, or an other (optimization) method should be used.

Two iterative optimization methods were discussed to produce a power density profile with positive power intensities only. The method of simulated annealing produced a small value of the object function, but resulted in a power density profile with numerous spikes. This is the result of the fact that heating of a work piece with a moving laser beam can be considered as an integrating operation or low pass filtering of the density profile.

It was shown that iterative spatial filtering of the power density profile, as calculated by the inverse heat conduction problem, produced a feasible and smooth power density profile. In this approach, total power of the density profile was linearly adjusted corresponding to the ratio between the desired maximum temperature and the calculated maximum temperature.

6 Acknowledgements

The comments and suggestions of Ferdi van der Heijden from the Laboratory for Measurement and Instrumentation of the University of Twente are greatly acknowledged.

References

[1] R.C. Crafer and A.P. Mackwood. Flexible 2D CW laser surface treatment model. *Lasers in engineering*, pages 241–249, 1999.

[2] T. Rudlaff, W. Bloehs, F. Dausinger, and Hügel. Hardening with CO_2-lasers and flexible beam shaping optics. In *Proceedings of the LAMP'92*, pages 673–677, 1992.

[3] J. Li, J. Merlin, J. Chen, and Z. Fan. Quick approximate calculation on the transient temperature field of laser heat treatment. *Chinese journal of lasers*, B6(3):280–288, 1997.

[4] J.C. Li and L. Yuan. Mathematical method for optimizing the process of heat treatment with powerful lasers. *Lasers in engineering*, 2:239–245, 1994.

[5] J. Li, Q.H. Chen, and J. Merlin. évaluation rapide du champ de température et de la forme de lase zone traitée lors d'un traitement superficiel de materiaux métalliques avec un faisceau laser de puissance. *Journal de physique III France*, 6:1293–1306, 1996.

[6] H.S. Carslaw and J.C. Jaeger. *Conduction of heat in solids*. Clarendon Press, Oxford, U.K., 1959.

[7] R.N. Bracewell. *The Fourier transformation and its applications*. McGraw-Hill, New York, U.S.A., 1986.

[8] J. Meijer, R.B. Kuilboer, P.K. Kirner, and M. Rund. Laser beam hardening: transferability of machining parameters. In *Proceedings of the LANE'94*, volume 1, pages 243–252, 1994.

[9] F.J. Harris. On the use of windows for harmonic analysis with the discrete Fourier transform. *Proceedings of the IEEE*, 66(1), 1978.

[10] G.R.B.E. Römer. *Modelling and control of laser surface treatment*. PhD thesis, University of Twente, Enschede, the Netherlands, 1999.

[11] A. Brandt and A.A. Lubrecht. Multilevel matrix multiplication and fast solution of integral equations. *Journal of computational physics*, 90:348–370, 1990.

[12] W.H. Press, B.P. Flannery, S.A. Teukolsky, and W.T. Vetterling. *Numerical recipes in Pascal*. Cambridge University Press, 1989.